FINAL REPORT
Prof. Yuri Aristov (Boreskov Institute of Catalysis SB RAS)
Visit to ITAE-CNR from April 17 till May 2, 2013 (Short Term Mobility Call)

Adsorption chillers (AC) are about to appear in the market [1], and optimization of their performance is of prime importance to make them more competitive with absorption and compression machines. According to the visit program, the research activity was focused on two lines:

- study of the effect of "adsorbent – heat exchanger" configuration and its optimization;
- study of the adsorbent properties by using combined TG-DSC technique.

1. Study of the effect of "adsorbent – heat exchanger" configuration

It is certain that the properties of the integrated unit "Adsorbent – Heat Exchanger" (Ad-Hex) determine the dynamic behaviour of adsorption chillers (AC) [2]. The AC dynamics is a complex process that can be affected by the Ad-Hex design (geometry), adsorbent configuration (loose grains or coating), grain size, layer thickness, flow rate, condenser/evaporator efficiency, etc. Here we focus on studying the loose grains configuration that is shown to be sufficiently efficient from the dynamic point of view [3, 4]. This configuration has already been comprehensively studied by a Large Temperature Jump method (LTJ) [5]. This method was intently developed to imitate conditions of AC isobaric stages when the ad-/desorption process is initiated by a fast drop/jump of temperature of a metal support (HEx fin) on which the adsorbent is located. It was primarily realized in a "constant volume – variable pressure" apparatus [5] (a volumetric LTJ or V-LTJ further on). The following main findings have been reported before [2, 3]:

(a) The initial part (60-90%) of sorption process follows an exponential kinetics and can be characterized by a single characteristic time τ. This is valid for various adsorbents [5, 6], grain sizes [6, 7], number of layers [8], and boundary conditions [7].

(b) A concave isobar is profitable for desorption, while a convex one - for adsorption [9].

(c) The isobaric adsorption stage of AC cycle is slower than the isobaric desorption stage [7].

(d) For a multi-layer configuration of the adsorbent bed of Fuji silica RD, the LTJ sorption dynamics is invariant with respect to the ratio <heat transfer surface area/adsorbent mass> = S/m [8]. For relatively small silica grains ($d < 0.8$ mm) and (S/m) > 1.0-1.5 $\mathrm{m^2/kg}$, a "lumped" regime is observed. Under this mode, the following linear dependence is valid

$$W_{max}\ [\mathrm{W/kg}] = A\Delta T_{max}\ (S/m)\ [\mathrm{m^2/kg}], \qquad (1)$$

where $A \approx 120\ \mathrm{W\ m^{-2}\ K^{-1}}$ for adsorption and $280\ \mathrm{W\ m^{-2}\ K^{-1}}$ for desorption runs regardless the silica grain size. It gives an upper-bound estimate of the power generated at AC ad- and desorption stages.

It is worthy to mention that the V-LTJ experiments are performed under conditions that are somewhat ideal as compared with those in real AC units. Indeed, adsorbent grains are located as *n* layers on a flat metal support (a primary fin) that is directly contacted with a heat carrier (Fig. 1). For such a configuration, only three main resistances are deemed to be important, namely, a) the contact heat transfer resistance between the metal support (HEx fin) and the granular adsorbent bed, b) the heat transfer resistance in the granular adsorbent bed, and c) the intrapartical diffusional resistance. The heat transfer between the metal support and the heat carrier is organized in a very effective way, and this resistance can be neglected at V-LTJ tests (indeed, change in temperature of the metal support is faster than 10 s). All other heat and mass transfer resistances can be neglected as well.

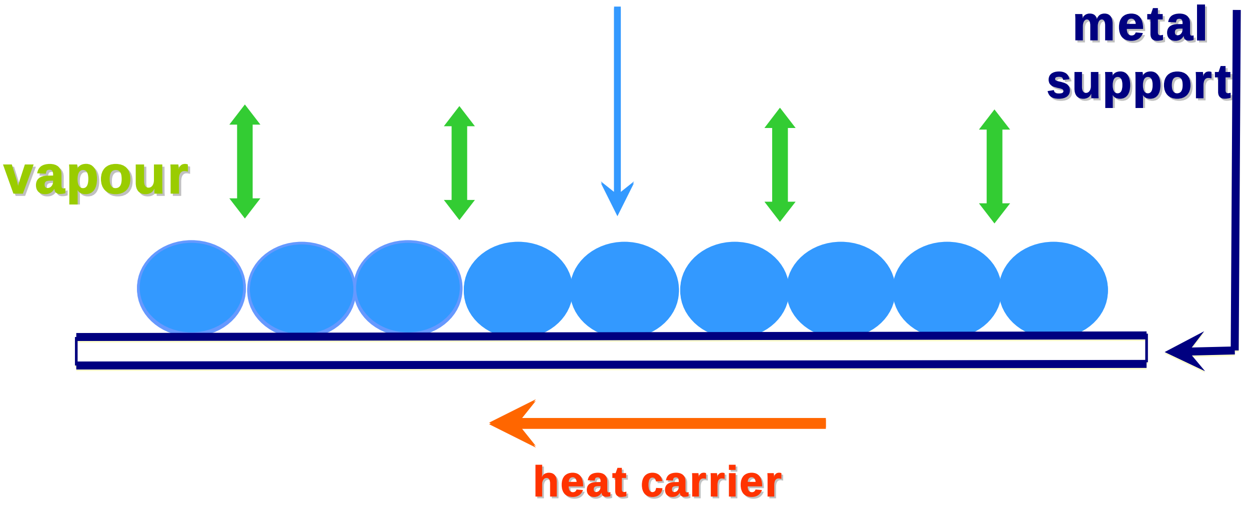

Fig. 1. Schematics of the V-LTJ method with a loose grains configuration.

These other resistances are, at least, but not last, as follows:

- heat transfer through the secondary fins surface can be not enough efficient;
- finned tube configuration with granulated adsorbent layer may suffer from intergrain mass transfer resistance that significantly increases for smaller grains and narrower gap between fins;
- additional mass transfer resistance can be due to a metal net that is used to fix adsorbent grains inside the fins;
- low speed or/and improper distribution of cooling/heating liquid that restricts the power (effect of the carrier flux);
- reduction of the adsorption rate due to the presence of residual gas (air);
- evaporator/condenser power does not fit the power of adsorption/desorption process.

Unfortunately, the V-LTJ can not be used to study the effect of these resistances because the mass of tested sample has to be less than 0.5 g. Therefore, generalization of the LTJ method to much bigger configurations, which represent real A-HE units of real AHTs, is strictly necessary as was suggested in [10]. The representative piece of a particular A-HE configuration can be a single adsorber module or its proper part (see Fig. 2).

a **b**

Fig. 2. a - View of the representative pieces of HEx units (two units, that are closer, have been studied in this work); b – HEx-1 filled with the FAM Z02 grains of 0.30-0.35 mm size and covered with a net (0.12 mm cell).

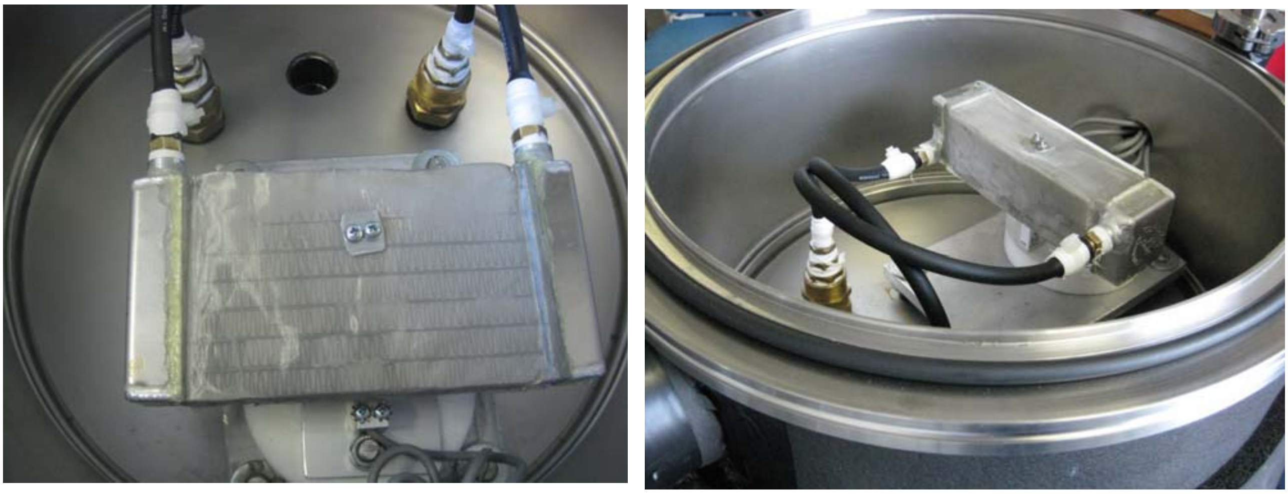

a **b**

Fig. 3. View of HEx-1 (a) and HEx-2 (b) installed in the G-LTJ unit.

In this study, a gravimetric version of the Large Temperature Jump method (G-LTJ) was applied to evaluate the influence of several mentioned parameters on the dynamic performance of Ad-HEx units. The G-LTJ version has recently been developed in ITAE-CNR [11]. Temporal evolution of the water uptake/release under conditions of isobaric ad-/desorption stages is directly measured by a micro-weighing system able to detect a weight of up to 500 g. In this case, a small

HEx or its part can be directly placed in the measuring cell. Details of the measurements can be found below.

The kinetic tests have been performed to answer the following main questions:

- Weather the ad-/desorption dynamics is invariant with respect to the (S/m)-ratio?
- What is the effect of the adsorbent grain size?

Preliminary analysis of several "secondary" questions

- Does the flow rate of the heat carrier affect the Ad-Hex operation?
- Does the condensed/evaporator affect the Ad-Hex operation?
- Does the adsorber thickness affect the Ad-Hex operation?

is also performed. All the data obtained for prototypes of real Ad-Hex units are compared with the "ideal" ones measured by the V-LTJ in BIC RAS (Novosibirsk, Russia).

We have studied two small Ad-HEXs (Fig. 2) with different thicknesses and almost equal ratio $(S/m) \approx 2.7 \pm 0.2$. Their geometry closely reproduces the geometry of the real flat tube finned Ad-HEx unit that was studied, for instance, in [12]. We filled it with loose grains of AQSOA FAM Z02 with the size of 0.30-0.35 and 0.60-0.71 mm.

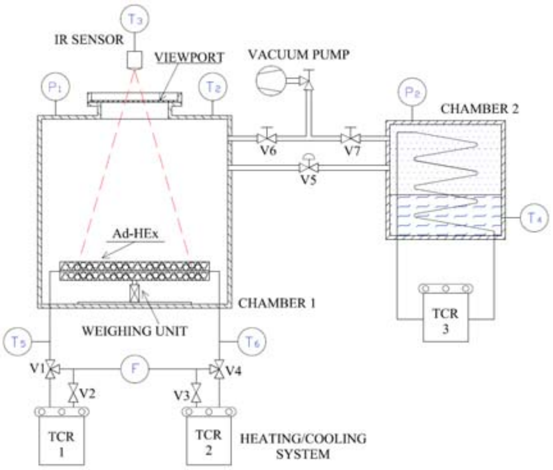

Fig. 4. Schematic layout of the G-LTJ measurement apparatus.

1.1. Experimental

1.1.1. Apparatus

A new experimental apparatus consists mainly of two vacuum chambers (Fig. 4). The first one is the measuring cell in which the Ad-HEx unit is connected both to a hydraulic heating/cooling system and to a supporting weighing unit. The latter consists in a load cell able to follow the weight evolution in a mass absolute range of 4-500g with the accuracy of 0.1 g and a time response faster than 0.1 s. The measuring cell is connected, through automatic valve V5, to chamber 2 that can operate as an evaporator or condenser. Both the Ad-HEx temperature and evaporator/condenser temperature can be managed by circulating thermal baths TCR1-TCR3. The flow rate of external heat transfer fluid can be regulated acting on the pumps speed, so that three heating/cooling scenarios might be realized (1.4, 2.0 and 2.8 l/min). All the relevant physical parameters (pressures, temperatures, flow rate) are acquired in real time each 1 s through a dedicated acquisition data system and displayed by a friendly software interface, specifically developed in the LABVIEW environment.

1.1.2. Test procedure

First, the adsorbent was equilibrated at initial conditions that corresponded to (12.2 mbar and 66°C) for adsorption and (42.2 mbar and 46°C) for desorption (see Fig. 5). Then, a fast temperature jump from 46 to 90°C was performed to initiate the isobaric desorption of water vapour. Similarly, the isobaric adsorption was initiated by a fast temperature drop from 66 to 30°C. This jump/drop was similar to that occurring in a real AHT. This causes a variation of the sample weight that directly corresponds to the water ad/desorbed. The pressure value is almost constant as chamber 2 and its internal coil heat exchanger were suitably designed to fit the requested evaporation/ condensation rate.

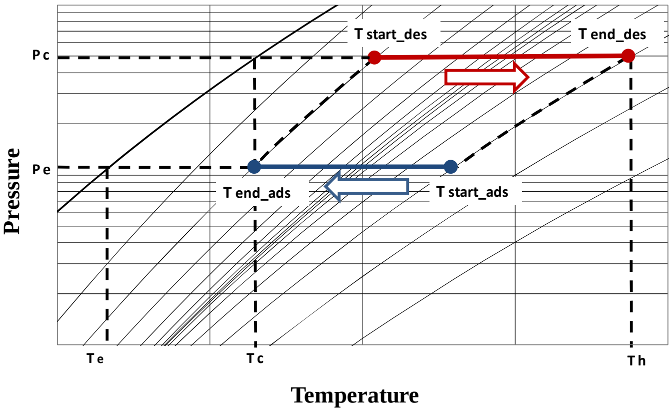

Fig. 5. Isosteric sorption chart for FAM-Z02 with the adsorption (blue line) and desorption (red line) routes.

1.1.2. Ad-HEx units tested

The finned flat-tube heat exchangers HEx1 and HEx2 represent a small scale version of the common air-cooled automotive HEx. It was proposed in the past for high power density adsorbers with adsorbents both in form of grains and in consolidated layers. It has been realized in aluminum with the same finned pack type (based on triangular louvered fins spaced 360 fins/m) and has been specifically designed keeping constant the (S/m) ratio and the HEx length (L), while the thickness was varied between 22 and 40 mm.

Table 1 displays the main features of the adsorbers analyzed: all the values reported are related to the finned pack. The average heat exchange area is 0.215 m^2 and the mean mass value is about 87 g, realizing the (S/m) ratio 2.75 ± 0.05.

Table 1. Characteristics of the tested HEx units.

Name	Lenght	Height	Thickness	Fins rows	S [m^2]	M_{metal} [kg]	S/ M_m	M_{ads} [kg]	S/m_{ads}
HEx 1	120	80	22	8	0.234	0.1615	1.45	0.084	2.8
HEx 2		40	40	4	0.208	0.135	1.54	0.090	2.7

For HEx 2, two of the four fins rows are external and from one side do not contact with the primary tubes. For this reason, we install two layers of silicon rubber (the thickness L = 1.5 mm) on the external sides to thermally isolate them from the environment. This permits to reach a heat transfer resistance of $(2L/\lambda) = (0.003\ m)/(0.2\ W/mK) = 0.015\ m^2K/W$ from each side.

2. Results and discussion

2.1. Ad-/desorption dynamics at "ideal" conditions of the V-LTJ method

We, first, report the dynamic data that have been obtained by the V-LTJ in BIC RAS (Novosibirsk, Russia) for water ad- and desorption on FAM-Z02 (the grain size 0.30-0.35 nm). These data will be used as reference data as well as an upper limit of the sorption rate. A two-layer configuration that is characterized by (S/m) = 2.4 was studied to imitate a proper ratio (S/m).

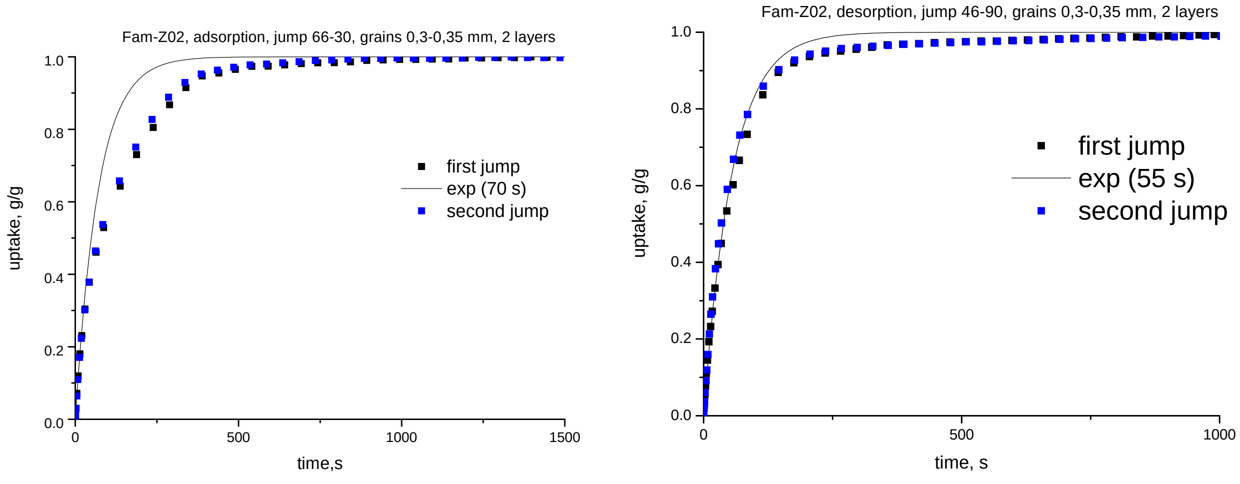

a **b**

Fig. 6 Dimensionless curves of isobaric water adsorption at 12.2 mbar (a) and desorption at 42.0 mbar (b) for FAM-Z02 loose grains of 0.30-0.35 mm size. Two layers configuration (*S/m* = 2.4). The temperature drop is 66-30°C and the jump is 46-90°C.

Adsorption kinetic curves were measured for isobaric adsorption at 12.2 mbar as well as for isobaric desorption at 42.0 mbar. For the first process the dynamics can be described by an exponential equation with the characteristic time $\tau_{ads} \approx 70$ s up to at the dimensionless conversion $\chi < 0.5$ (Fig. 6a). At $\chi > 0.5$ the process becomes slower than the exponential one. For the isobaric desorption run at 42.0 mbar, the release curve is exponential up to at the dimensionless conversion $\chi < 0.9$ (Fig. 6b). The characteristic desorption time τ_{des} is c.a. 55 s.

We shall consider the characteristic times $\tau_{ads} = 70$ s and $\tau_{des} = 55$ s as reference points that correspond to the ideal situation when the only resistances are the heat transfer to and in the adsorbent bed and the intraparticle mass transfer.

2.2. Ad-/desorption for Ad-HEx1 studied by the G-LTJ method

For all the performed tests, the shape of the curves "sorption uptake/release" vs. "time" was nearly exponential and can be described by a single characteristic time τ. This time is used further on for comparing with the "ideal" case and analyzing the effect of various parameters.

Since there are many parameters that can affect the ad-/desorption dynamics, the basic settings are as follows: the flow rate 2.8 l/min, the water volume in the condenser/evaporator 1.5 liters, tubes precooling/preheating, fast evacuation of the evaporator and the chamber before each temperature drop/jump.

2.2.1. Grains of the 0.30-0.35 mm size

All the characteristic times obtained are displayed in Table 2. It is clear from this Table that both ad- and desorption dynamics are well reproducible. The average characteristic adsorption time is $\tau_{0.8} = 113$ s, while for desorption it is much shorter $\tau_{0.8} = 76$ s. Both these times are longer than the "ideal" ones, and the ratio is (113/70) = 1.6 for adsorption and (76/55) = 1.38 for desorption. Surprisingly, the tested Ad-HEx possesses quite efficient performance that is only 40-60% lower than the "ideal" one. One of the possible reasons is that the efficiency of secondary fins is lower than that of primary ones, however, more study is necessary to clarify this issue.

Table 1. Characteristic times $\tau_{0.8}$ and $\tau_{0.95}$ for at various experimental conditions. Grain size 0.30-0.35 mm. Ad-HEx1.

File	T_{in}	T_{fin}	$\tau_{0.95}$	$\tau_{0.8}$
test 2 18.04.2013 90-30-10 ads 66-30 fr 3 heater on	*67*	*30*	***105***	***114***
test 1 19.04.2013 90-30-10 ads 66-30 fr 3 heater on bis	67	30	**101**	**113**

test 3 19.04.2013 90-30-10 des 46-90 fr 3 heater on	47	91	**75.7**	**76.7**
test 4 19.04.2013 90-30-10 des 30-90 fr 3 heater on D.C.	47	91	**72.4**	**76.0**

2.2.1. Grains of the 0.60-0.71 mm size

Similar data for AD-HEx1 filled with bigger grain of FAM-Z02 are presented in Table 3. Again, the ad- and desorption dynamics are reproducible. The average characteristic adsorption and desorption times are $\tau_{0.8}$ = 124 s and 82 s. Both these times are somewhat longer for bigger grains, and the ratio ($\tau_{0.6mm}/\tau_{0.3mm}$) is (124/113) = 1.1 for adsorption and (81/76) = 1.08 for desorption. It means that the increase in the grain size by a factor of 2 gives only little effect on both adsorption dynamics and desorption one. This is in good agreement with the "lumped" regime observed by the V-LTJ for the Fuji silica RD in [8].

Table 3. Characteristic times $\tau_{0.8}$ and $\tau_{0.95}$ for at various experimental conditions. Grain size 0.60-0.71 mm. Ad-HEx1.

File	T_{in}	T_{fin}	$\tau_{0.95}$	$\tau_{0.8}$
test 5 26.04.2013 90-30-10 ads 66-30 fr 3.5 heater on	*67*	*30*	***121***	***124***
test 6 26.04.2013 90-30-10 ads 66-30 fr 3.5 heater on	*67*	*30*	***121***	***126***
test 13 29.04.2013 90-30-10 ads 66-30 fr 3.5 heater on	*67*	*30*	**116**	**122**
test 8 29.04.2013 90-30-10 des 46-90 fr 3.5 heater on	91	47	**88**	**85**
test 10 29.04.2013 90-30-10 des 46-90 fr 3.5 heater on	91	47	**80**	**78**

2.3. Ad-/desorption for Ad-Hex2 studied by the G-LTJ method

It is worthy to remind that HEx2 has the same (*S/m*)-ratio, while its thickness is 40 mm instead of 22 mm for HEx1 (see Figs. 2 and 3). All the experiments are performed with the FAM grains of 0.30-0.35 mm size (see Table 4).

The characteristic desorption time for this Ad-HEx (80 s) is almost equal to that (76 s) for Ad-HEx1 filled with the same grains. It confirms the conclusion of refs. [3, 4, 11] that at equal values of (S/m) the sorption dynamics are very close. It is true if the process is limited by heat transfer as it is a case at the "lumped" sorption mode revealed in [4].

Very strong slowing down was observed for isobaric adsorption stage so that the ratio (τ_{HEx2}/τ_{HEx1}) = (186/113) = 1.65. In our opinion, this is because the adsorption rate is limited by the intergrain mass transfer resistance. Indeed, this resistance may significantly increase when small grains occupy a long and narrower gap between fins. For Ad-HEx2, the average channel thickness = 2 mm, the width = 9 mm and the length = 40 mm, each channel being filled with adsorbent grains of size d = 0.33 mm. It means that 6 grains are located between two secondary fins and 25-30 grains – between two primary fins. In the future, it is necessary to assess a mass transfer resistance in such a narrow channel with a few number of adsorbent grains. At the moment, only brief estimation based on the equation for the gas permeability of a porous medium can be done. According to the classical model, the permeability reduces for smaller grains as d^2, hence, it can be significantly low for smaller grains. For the desorption run, this slowing down is not observed, probably, because of a higher pressure gradient along the channel which intensifies the matt transport. More experiments are necessary to check this hypothesis.

When HEx2 is only partially filled with the same adsorbent grains (c.a. 2/3 of the complete filling, in average), the adsorption time reduces to 123 s (see the last line of Table 4). It is close to 113 s that is a "normal" time for the tested HEx with the ration (S/m) = 2.7.

Table 4. Characteristic times $\tau_{0.8}$ and $\tau_{0.95}$ for at various experimental conditions. Grain size 0.30-0.35 mm. Ad-HEx2.

File	T_{in}	T_{fin}	$\tau_{0.95}$	$\tau_{0.8}$
test 1 30.04.2013 90-30-10 ads 66-30 fr 3.5 heater on	*67*	*30*	***188***	***190***
test 3 30.04.2013 90-30-10 ads 66-30 fr 3.5 heater on	*67*	*30*	***178***	***183***
test 6 30.04.2013 90-30-10 ads 66-30 fr 3.5 heater on	*67*	*30*	**178**	**185**
test 9 30.04.2013 90-30-10 des 46-90 fr 2,8	91	47	**79**	**79**
test 15 30.04.2013 90-30-10 des 46-90 fr 2.8	91	47	**82**	**82**
test 7 24.04.2013 90-30-10 ads 67-30 fr 3 heater on ter	91	47	**113**	**123**

Hence, the adsorber thickness can strongly affect operation of the studied Ad-Hex even if the (S/m) ratio remains constant. Isobaric adsorption at low vapour pressure is mostly sensitive to the HEx thickness. This effect is caused by the intergrain mass transfer resistance. In has to be further studied, e.g. by inserting bigger grains to HEx2 or smaller grains to HEx1.

Several other "secondary" effects are also briefly evaluated by the present G-LTJ method as discussed below.

2.4. Effect of the flow rate of the heat carrier

In fact, during these tests we have not focused on studying this effect. Nevertheless, it has likely been observed during desorption phase at Ad-HEx2 filled with 0.30-0.35 mm grains (Table 5). Indeed, the desorption time reduces as (95/80) = 1.19 if the flow rate is 1.4 l/min, while for faster flow rates (2.0 and 2.8 l/min) it is constant (and "normal"). As the majority of the runs are performed at the flow rate 2.8 l/min, there is not limitation due to this factor.

Table 5. Characteristic times $\tau_{0.8}$ and $\tau_{0.95}$ for at various flow rates. Grain size 0.30-0.35 mm. Ad-HEx2.

File	Flow rate, l/min	$\tau_{0.95}$	$\tau_{0.8}$
test 13 30.04.2013 90-30-10 des 46-90 fr 1.4	1.4	***93***	***95***
test 11 30.04.2013 90-30-10 des 46-90 fr 1.4	1.4	**92**	**95**
test 14 30.04.2013 90-30-10 des 46-90 fr 2.0	2.0	**77**	**80**
test 15 30.04.2013 90-30-10 des 46-90 fr 2.8	2.8	**82**	**82**
test 9 30.04.2013 90-30-10 des 46-90 fr 2,8	2.8	**79**	**79**

2.5. Effect of the condensed/evaporator efficiency

This effect is revealed when the flux of water through the condenser was significantly reduced. As a result the desorption kinetics at high pressure was essentially slower that at normal condenser operation.

3. Study of the adsorbent properties by using combined TG-DSC technique

The experimental measurements have been carried out by means of a modified DSC-TG apparatus. It is a Setaram Labsys-Evo, equipped with a standard DSC rod, having a resolution of 10 μW, and a TG probe characterized by 0.02 μg of resolution and 0.02 mg of accuracy. The thermo-gravimetric system is able to reach up to 800°C, and it has been modified in order to work under saturated water vapour pressure conditions. The following Fig. 1 represents the schematization of the thermo-gravimetric apparatus. It is mainly composed of a testing chamber (TestC), in which the sample (S) and the reference (R) crucibles are located. The furnace cooling rate is controlled by means of an external thermo-cryostat (TC2). The testing chamber can be evacuated, during the regeneration of the sample, employing a vacuum pump (VP), which is connected to the chamber by means of two vacuum valves arranged in parallel (V2 and V3), one of which is a needle valve (V3), employed during the first evacuation stages in order to avoid the elutriation of the sample. Moreover, the generation of the water vapour is obtained by means of an glass evaporator (Evap) whose temperature is controlled by an external thermo-cryostat (TC1). Finally, both the chamber pressure and the evaporator pressure are continuously monitored by means of two dedicated sensors (P).

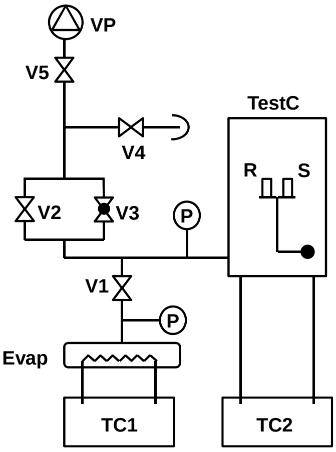

Fig. 7: Schematic drawing of the thermo-gravimetric apparatus installed at the CNR ITAE labs.

The following Fig. 8 represents the installed apparatus at the CNR ITAE laboratories. Here, the testing chamber (1), the two pressure sensors employed to monitor both the chamber pressure (2) and the evaporator pressure (3), and the evaporator itself (4) can be recognized.

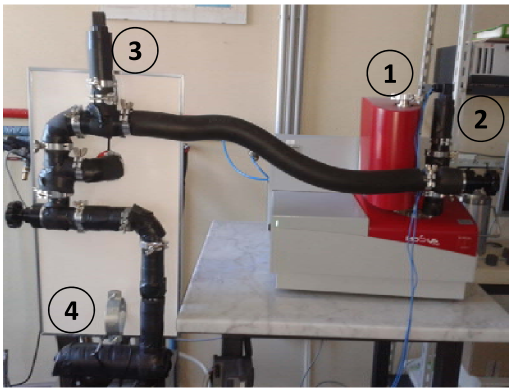

Fig. 8: Picture of the thermo-gravimetric apparatus installed at the CNR ITAE labs: 1) Testing chamber, 2) and 3) Pressure sensors 4) Glass evaporator.

Testing procedure

The following flow chart (Fig. 9) reports the main phases of the employed testing procedure for the adsorption capacity characterization of the selected materials. The methodology was derived from the standardized protocol of characterization recently developed and proposed by Henninger et al. [13].

The sample is weighted by means of an external microbalance having a resolution of 1 µg. Usually about 20 mg are loaded into the crucible. Afterwards, the sample is put inside the measurement chamber and it is slowly evacuated, in order to avoid the sample elutriation, by means of a rotary vacuum pump, at ambient temperature. Then, it is heated up to 150°C under continuous evacuation for 8 h, in order to get the dry sample. Finally, the water vapour is admitted inside the measurement chamber, by means of an external evaporator whose temperature is set constant employing a thermo-cryostat (TC1). The isobar is measured recording 9 equilibrium points, with temperature ranging between 150°C and 30°C.

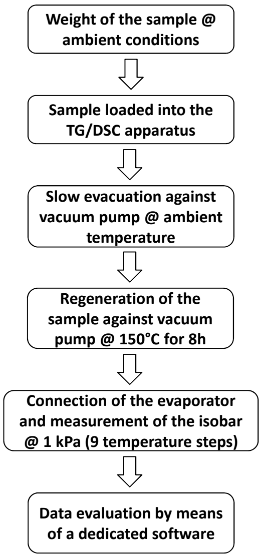

Fig. 9: Flow chart of the main testing procedure phases.

The following Fig. 10 reports a dynamic evolution obtained during the testing of the AQSOA FAMZ02. In the picture the temperature evolution (red line), the weight (green line) and the heat flux (blue line) can be recognized. Of course, by integrating each heat flux peak, it is possible to evaluate the integral heat of adsorption associated to the adsorption phenomena.

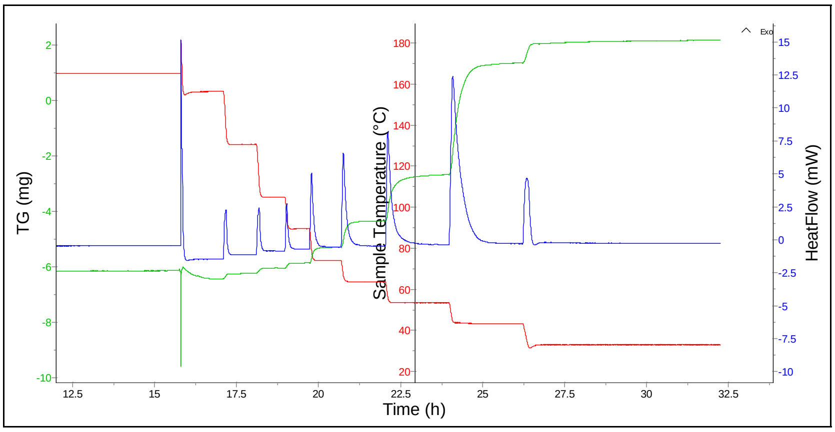

Fig. 10: Dynamic evolution of temperature (red) weight (green) and heat flux (blue), obtained during an adsorption test carry out over the AQSOA FAMZ02 by means of the TG-DSC apparatus available at the CNR ITAE lab.

Starting from each equilibrium point, the complete isobar was evaluated. The Fig. 11 reports a comparison between the isobars obtained by means of the new apparatus available at the CNR ITAE (Labsys Evo) and by means of the standard microbalance Cahn C2000. The evolutions result to be quite comparable each other, which confirms the applicability of the new apparatus for the isobaric equilibrium measurements.

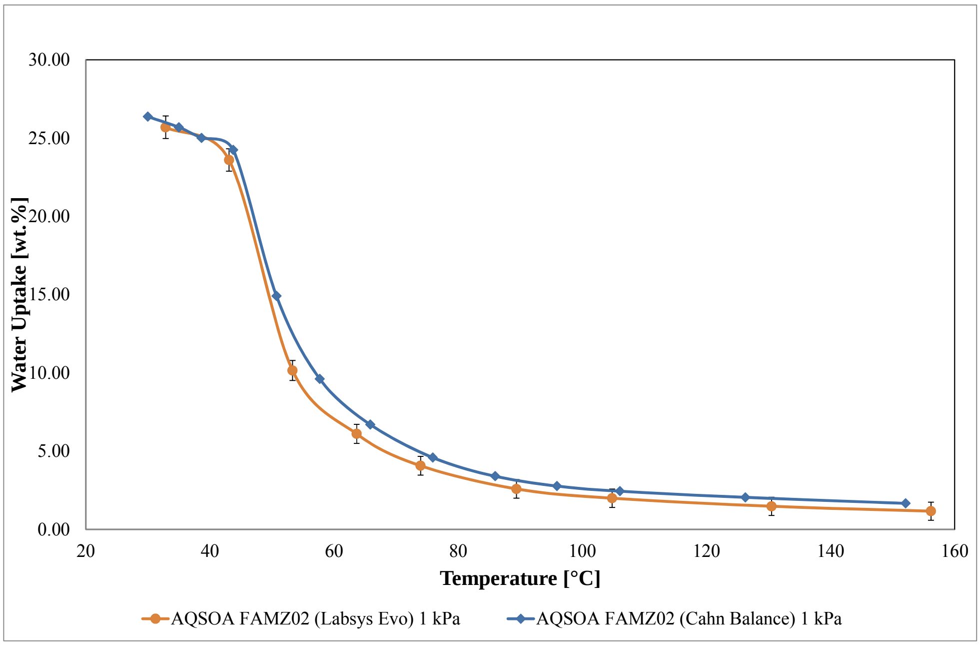

Fig. 11: Comparison between the equilibrium isobaric curve at 1 kPa, for AQSOA FAMZ02 measured by means of the recently installed Labsys Evo apparatus (orange) and by means of the standard Cahn C2000 microbalance (blue).

Further investigations will be devoted to the evaluation of the adsorption enthalpy measurements repeatability and to investigate thermodynamic properties of other adsorbent materials, aiming at the evaluation of the most promising for different AHT working conditions.

Literature

---

1 Jakob U, Kohlenbach P. Recent Developments of Sorption Chillers in Europe, IIR Bulletin, 2010, pp. 34-40.

2 Aristov Yu.I. Optimal adsorbent for adsorptive heat transformers: Dynamic considerations. Int. J. Refrig., 2009, vol. 32, pp. 675-686.

3 Yu.I. Aristov, Experimental and numerical study of adsorptive chiller dynamics: a loose grains configuration, Appl. Thern. Engn., 2013 (accepted).

4 Yu. I. Aristov, I. S. Girnik, I. S. Glaznev, Optimization of adsorption dynamics in adsorptive chillers: Loose grains configuration, Energy, 2012, v. 46, pp. 484-492.

5 Aristov YuI, Dawoud B, Glaznev IS, Elyas A, A new methodology of studying the dynamics of water sorption under real operating conditions of AHPs: Experiment. *Int. J. Heat Mass Transfer*, Vol. 51, 4966-4972, 2008.

6 Gordeeva LG, Aristov YuI, Composite sorbent of methanol "LiCl in mesoporous silica gel" for adsorption cooling: dynamic optimization. *Energy* 2011;36:1273-1279.

7 Glaznev IS, Aristov YuI, The effect of cycle boundary conditions and adsorbent grain size on dynamics of adsorption chillers. *Int. J. Heat & Mass Transfer*, Vol. 53, 1893-1898, 2010.

8 Aristov YuI, Girnik IS, Glaznev IS, Optimization of adsorption dynamics in adsorptive chillers: Loose grains configuration, Energy, 2012, v. 46, pp. 484-492.

9 Glaznev IS, Ovoshchnikov DS, Aristov YuI, Kinetics of water adsorption/desorption under isobaric stages of adsorption heat transformers: the effect of isobar shape. *Int. J. Heat&Mass Transfer* 2009, 52: 1774-7.

10 I.S. Glaznev, Yu.I. Aristov, Dynamic Aspects of Adsorptive Heat Transformation, In book: "Advances in Adsorption Technologies", 2010, Eds. B. Saha and K.S. Ng; Nova Science Publishers, ISBN: 978-1-60876-833-2, p. 157.

11 A. Sapienza, S. Santamaria, A. Frazzica, A. Freni, Yu.I. Aristov, A new gravimetric version of the large temperature jump method: loose adsorbent grains over a flat plate heat exchanger, Appl. Energy, 2013 (submitted).

12 Yu.I. Aristov, A. Sapienza, A. Freni, D.S. Ovoschnikov, G. Restuccia, Reallocation of adsorption and desorption times for optimizing the cooling cycle parameters, Int. J. Refrig., 2012, v. 35, N 3, pp. 525-531.

13 Henninger, S. K., A. Freni, L. Schnabel, P. Schossig, G. Restuccia. 2011. Unified water adsorption measurement procedure for sorption materials. In International Sorption Heat Pump Conference, 513-522. Padova, Italy: IIR/AICARR.